Experimental Study and Finite Element Analysis on the Seismic Properties of Stiffened CHS Bracket to CHS Beam Connections under Cyclic Torque

Chen Yiyi[1], Jia Liangjiu[2], Meng Xiande[3]

[1] *Professor, Dept. of Civil Engineering ,Tongji University, Shanghai, China*
[2] *Master, Dept. of Civil Engineering ,Tongji University, Shanghai, China*
[3] *Doctor, Dept. of Civil Engineering ,Tongji University, Shanghai, China*
Email: lungo786@hotmail.com

ABSTRACT :

An experimental investigation into the seismic properties of the typical joints used in the 610m high Guang-zhou New TV tower has been conducted. All specimens consist of a concrete-filled CHS column (circular), a steel bracket, two steel circular hollow section (CHS) beams and two steel CHS bracings. Whereas the members are not coplanar, which result in that the bracket is subjected to combined torque and small moment. The stiffened bracket is used to connect the column and the beams that are directly welded to the bracket. The present paper mainly presents the experimental and finite element analysis (FEA) results of the bracket to beam connection. Stiffened connections with various dimensions are compared with the unstiffened ones to find out the effect of stiffeners on the seismic properties of the connections. It is found that both the ultimate strength and the stiffness of the joints have been improved compared with the unstiffened joints. Meanwhile, a theoretical model indicates that the small moment has little effect on the seismic properties of the connections.

KEYWORDS: bracket to beam connection, tubular structure, seismic design, finite element

1. INTRODUCTION

1.1. General

Previous research concerned with the seismic design of tubular joints mainly focuses on the cases under axial or pure bending loads which may be summarized as follows: 23 complete tubular truss tests have been accomplished by Kurobane at Kumamoto University, Japan, in which four specimens have concrete-filled chords, four specimens are composite trusses with concrete slabs and two specimens are space trusses [1-3]. The research mainly focused on the interaction between the connections and the trusses. A number of tests on the cyclic behavior of the steel tubular structures have been carried out by Usami and his co-authors at Nagoya University, Japan [4], some strength and ductility formulas of steel box and pipe columns modeling bridge piers for seismic performance evaluation have been suggested. Eight specimens have been tested to study the cyclic behavior of the CHS T-joints by Wei Wang at Tongji University, China [5], four of which are under cyclic axial load and the other four are subjected to cyclic in-plane bending. The respective failure modes of the two cases are concluded and the method to calculate the ultimate strength of the CHS T-joints is suggested. Considerable research work has been done by Mohamed Elchalakani and his co-authors on the cyclic behavior of cold-formed hollow steel members at Monash University, Australia, and the slenderness limits of cold-formed CHS tubes under cyclic bending are established [6][7]. However, few researches on the connections under cyclic torque loading have been found.

1.2. Scope

As the development of new types of structures, there are many cases which are not covered by the codes. Therefore, experiments are required to investigate the hysteretic behavior of CHS connections. The typical joints of the six hundred and ten meters high Guang-zhou new TV tower have been tested under quasi-static cyclic loading. All specimens consist of concrete-filled CHS column (circular), a stiffened steel CHS bracket, two steel CHS beams and two steel CHS bracings. The members are not coplanar, thus a stiffened bracket is introduced to connect the column and the beams that are directly welded to the bracket, which results in that the bracket is subjected to combining torque and small moment as shown in Fig.1. The present paper mainly presents the experimental and FEA results of the bracket to beam connection. Stiffened connections with various dimensions are compared with the unstiffened ones to find out the effect of stiffeners on the seismic properties of the connections.

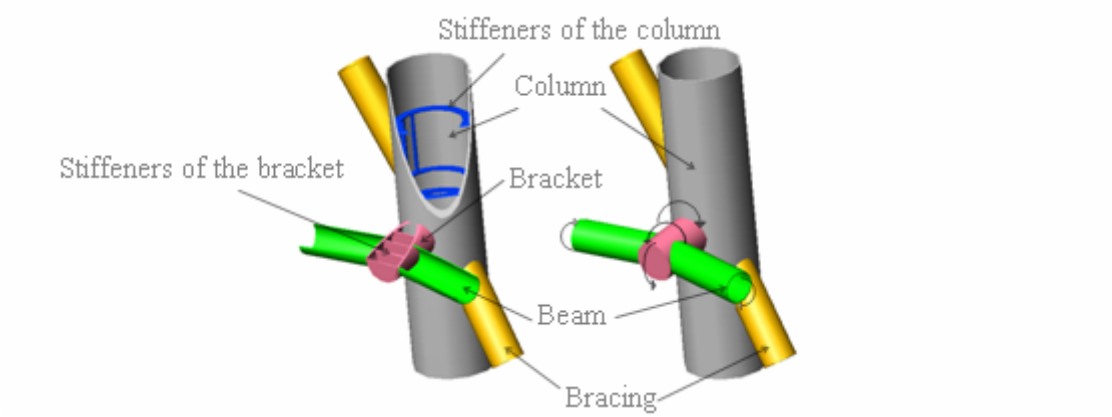

Figure 1 3D perspective view of typical joint

Nomenclature

d	Outside diameter of beam	T_y	Yield torque of bracket
D	Outside diameter of bracket	T_p	Plastic torque of bracket
M_{max}	Maximum moment of FEA beams	W_T	Section modulus of torsional rigidity
M_{ybe}	Yield moment of beam section	W_{ybr}	Yield section modulus of bracket
M_{ybr}	Yield moment of bracket section	W_{pbr}	Plastic section modulus of bracket
M_{pbe}	Plastic moment of beam section	α	Ratio of d and D
M_{pbr}	Plastic moment of bracket section	θ	Rotation of bracket section
P	Beam tip load	Δ	Neat beam tip deflection
P_p	Plastic beam tip load	Δ_y	Yield beam tip deflection
P_y	Yield beam tip load	τ	Shear stress
t_{br}	Thickness of bracket	σ	Normal stress
t_{be}	Thickness of beam	σ_r	Equivalent stress
T	Torque of bracket	σ_u	Ultimate stress
T_{max}	Maximum torque of FEA bracket	σ_y	Yield stress

2. EXPERIMENTAL PROGRAM

2.1. Material and Details for the Specimen

The mechanical properties of the steel obtained by coupon tests are listed in Table 1. The specimens are welded using continuous fillet welds. The nominal geometric dimensions of the specimens are also shown in Table.1, and the thickness of the stiffeners is 5 mm, which is the same as that of the beams. From the table, it can be seen that specimen HB has a stronger column than specimen HW, whereas the other members are of the same dimensions.

Table 1.1 Dimensions and mechanical properties of specimens

Specimens	Dimension	Outside diameter(mm)	Thickness (mm)	σ_y (MPa)	σ_u (MPa)	σ_u / σ_y
HB	Bracket	200	8	363	519	1.42
	Beam	159	5	343	475	1.39
	Column	402	10	364	525	1.44
HW	Bracket	200	8	363	519	1.42
	Beam	159	5	343	475	1.39
	Column	310	8	363	522	1.44

2.2.Test Setup

The specimens were tested in the Building Structural Research Laboratory, Tongji University.
Figure.2 shows the general arrangement of the test. The beam tips are bolted to two reaction linking CHS which is connected to the base of the ground. A loading beam is used to apply vertical and horizontal loads. The horizontal force is applied to generate a torque in the bracket, whereas the beams are subjected to bending.

2.3. Loading history

During the test, first a vertical compressive force of 2000kN was applied on the top of the loading beam by the vertical jack. Keeping the vertical compression constant, a cyclic horizontal force was applied on the loading beam until one of strain gauges on the joint yielded which is defined as yield displacement corresponding Δ_y .Then a typical column tip horizontal displacement controlled loading program was established by times of Δ_y .

3. TEST RESULTS AND DISCUSSION

3.1. Observations and Failure Modes

The test results given in the present paper are from a typical joint at the bottom (HB) of the TV tower, whereas a typical joint at the waist (HW) of the structure is also tested under reversed low cyclic loading. Joint HB sustained all loading steps up to and including half of the $14\Delta_y$ column tip

displacement cycles without significant damage. During the last set of the load reversals, a tiny weld cracking of the beam tips at the bracket wall was observed. Testing was stopped because the displacement limitation of the test setup was reached. From the test, it was found that the weld cracking happened after plastic moment of the beam was reached. While for joint HW, it failed due to the local buckling of the beam wall in compression. The failure modes of joint HB and HW are illustrated in Figure.3.

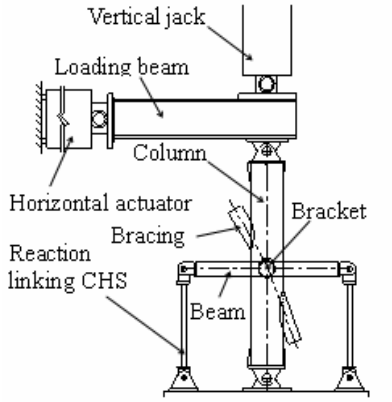

Figure 2 specimen and loading rig

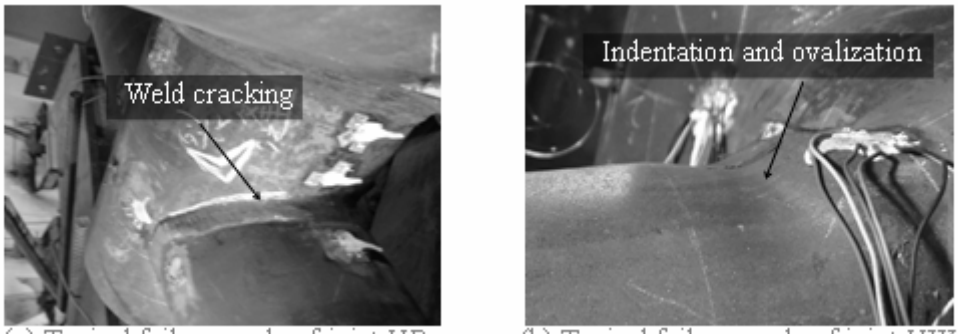

(a) Typical failure mode of joint HB (b) Typical failure mode of joint HW

Figure 3 Failure modes of specimens

3.2. Hysteretic curves of HB

The load versus relative displacement curves of the bracket and the torque versus relative rotation curves of the beam are shown in Figure.4 and Figure.5 respectively, where Δ is the neat beam tip displacement, and the deformation resulted by the rotation of the bracket has been subtracted. And P is the beam tip load. θ is the total rotation of the bracket section, and T is the torque which is obtained by multiplying P and the length of the beam.

From the curves, it can be seen that both the beam and the bracket reach their plastic resistance. The test also indicates that the stiffened CHS bracket has an excellent ductility under cyclic combining torque and small moment loading. The energy was mainly dissipated by cyclic yielding of the bracket and the beams.

For specimen HW, the stiffness of the column is much smaller than that of HB. When the vertical load is applied, the beams bear a large proportion of the load, so the load versus displacement curve of HW is not central symmetric. The ultimate beam tip load P and torque T of HW is higher than that of HB, for HB fails mainly due to the cracking of the welds, and the load drops rapidly after the cracks are formed. Whereas HW fails mainly due to the local buckling of the beam section, thus the maximum rotation of the bracket section is relative small.

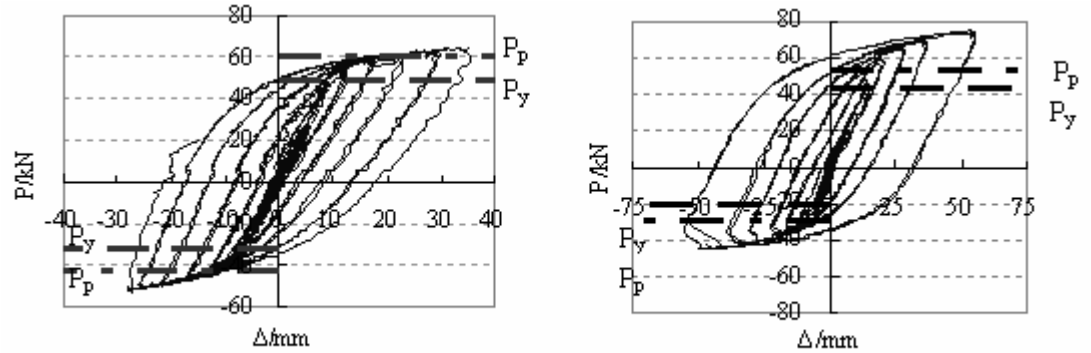

Figure 4 Load versus displacement curves for beams

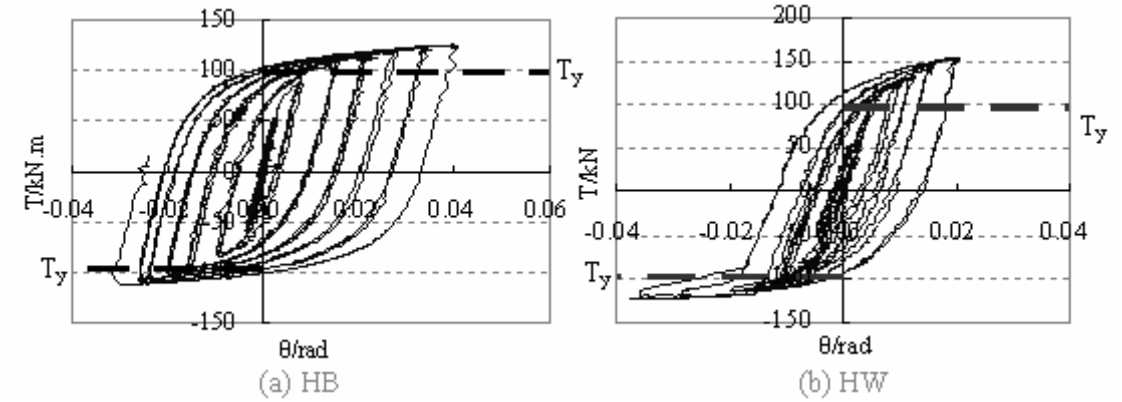

Figure 5 Torque versus rotation curves for brackets

4. PARAMETRIC ANALYSIS

4.1. Effect of the Small Moment on the Seismic Performance of the Bracket

According to material mechanics, the equivalent stress is:

$$\sigma_r = \sqrt{\frac{1}{2[(\sigma_1-\sigma_2)^2+(\sigma_2-\sigma_3)^2+(\sigma_1-\sigma_3)^2]}} \tag{4.1}$$

For the tubes, the wall thickness of which is relative small compared with its radius, it is assumed that the second principal stress: $\sigma_2 = 0$

Then,
$$\begin{pmatrix}\sigma_1\\ \sigma_3\end{pmatrix} = \frac{\sigma}{2} \pm 1/2\sqrt{\sigma^2+4\tau^2} \tag{4.2}$$

Where,
$$\sigma = \frac{M_{br}}{W_{ybr}} \tag{4.3}$$

$$W_{ybr} = \frac{\pi D^3}{32}(1-\alpha^4),\ \alpha = \frac{d}{D} \tag{4.4}$$

$$\tau = \frac{T}{W_T} \tag{4.5}$$

$$W_T = \frac{\pi D^3}{16}(1-\alpha^4) = 2W_{ybr} \tag{4.6}$$

Then, equivalent stress is: $\sigma_r = \sqrt{\sigma^2 + 3\tau^2} = \frac{1}{W_{ybr}}\sqrt{M_{br}{}^2 + 0.75T^2}$ (4.7)

Where σ is normal stress and τ is shear stress. W_{ybr} is the yield section modulus of the bracket section, whereas W_T is the section modulus of torsional rigidity.

The equivalent stress at the first yielded fiber is: $\sigma_r = \sigma_y$

When the moment at the free end of the bracket: M=0, the yield torque of the bracket section is:

$$T_y = \frac{2\sqrt{3}}{3} W_{ybr}\sigma_y \quad (4.8)$$

When the moment at the free end of the bracket: $M = 0.1M_{ybr} = 0.1W_{ybr}\sigma_y$, the yield torque of the section is:

$$T_y = \sqrt{0.99} \times \frac{2\sqrt{3}}{3} W_{ybr}\sigma_y \quad (4.9)$$

By comparison with equation (4.8) and (4.9) it can be concluded as: the existing small moment has little effect on the yield torque of the tubular section.

At the points where material is yielded, the equivalent stress is equal to:

$$\sigma_r = \sqrt{\sigma^2 + 3\tau^2} = \sigma_y \quad (4.10)$$

Then, $$\sigma = \sqrt{\sigma_y{}^2 - 3\tau^2} \quad (4.11)$$

where $$\tau = \frac{T}{W_T} \quad (4.12)$$

Thus the moment of the bracket is: $$M_{br} = W_{Pbr}\sigma = W_{Pbr}\sqrt{\sigma_y{}^2 - 3\tau^2} \quad (4.13)$$

And the plastic resistances of the section is:

$$T_p = W_T \frac{\sigma_y}{\sqrt{3}} \quad (4.14)$$

$$M_{pbr} = W_{pbr}\sigma_y \quad (4.15)$$

Hence, $$\frac{M_{br}}{M_{pbr}} = \frac{W_{pbr}\sqrt{\sigma_y{}^2 - 3\tau^2}}{W_{pbr}\sigma_y} = \frac{\sqrt{\sigma_y{}^2 - 3\tau^2}}{\sigma_y} \quad (4.16)$$

$$\frac{T}{T_p} = \frac{W_T\tau}{W_T\frac{\sigma_y}{\sqrt{3}}} = \frac{\sqrt{3}\tau}{\sigma_y} \quad (4.17)$$

Thus, the relationship between the moment and the torque of the tubular section is established as:

$$\left(\frac{M_{br}}{M_{pbr}}\right)^2 + \left(\frac{T}{T_p}\right)^2 = 1 \quad (4.18)$$

4.2. FEA Parametric Analysis

Four-node shell elements (element type SHELL181 in ANSYS) are used in the FE models. To study the respective influence on the seismic performance of the connection, four FE models with various dimensions are analyzed under cyclic loading. The geometric and theoretical mechanical properties of the models are listed in Table 4.1. A cyclic load is applied by the beam tip displacement.

The maximum FEA resistance is calculated as follows. The maximum beam moment, M_{max}, at the plastic hinge is equal to PL, where L is the length of the beams. The maximum torque of the bracket is T_{max}, which is equal to $2M_{max}$. As shown in Figure 6, the FEA bracket is under combining

flexural normal stress and torsional shearing stress. The moment applied on bracket is kept constant ($0.1\,M_{ybr}$) to simulate the case that bracket is subjected to a torque with a relative small moment under cyclic loading.

Table 4.1 Dimensions and results of FEA models

Case	Bracket			Beam				FEA results	
	D	t_{br}	T_y	d	t_{be}	M_{ybe}	M_{pbe}	T_{max}	M_{max}
J1s	200	10	107.6	160	8	47.7	63.8	192.6	96.3
J1u								154.4	77.2
J2s	200	4	47.1	100	10	20.0	28.1	53.2	26.6
J2u								4.4	8.7

J1s means stiffened joint J1, whereas J1u means unstiffened joint J1. All dimensions are expressed in mm, whereas all strength is expressed in kN.m .

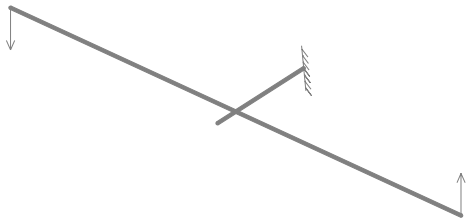

Figure 6 Boundary and loading conditions of joint

4.3. Effect of Stiffeners on the Seismic Performance of the Joint

It can be seen from Figure 7 and Figure 8 that the ultimate bearing capacity of the stiffened joints is enhanced compared with the unstiffened ones. It is also found that both the beam tip deflection and the rotation of the bracket are reduced significantly. Previous research also has shown that the unstiffened tubular joints may usually have lower capacity compared with adjacent members.

One of the main factors affecting the seismic performance of the joint is the load bearing capacity ratio T_y / M_{pbe}. If it is close to 2 and the strength of the joint is high enough, then the bracket and the beams will all yield, thus the energy dissipation capability of the joint is preferable, and the ductility of the joint is also improved to allow a structure to have a bigger deformation under a sever earthquake event. But if the ratio is much larger or smaller than 2, either the bracket or the beams will not yield even limit states are reached.

It can be seen from table.2 that T_y / M_{pbe} of J1 is close to 2 whereas for J2 it is bigger than 2. However, the performance of the unstiffened joint J2 is still undesirable. Both the beams and the bracket have not reached their plastic capacity. The FEA results also indicate that the low moment transferring capacity of the bracket wall will result in the premature failure of the joint. So even if T_y / M_{pbe} is bigger than 2, the strength and ductility of the joint must be satisfactory to ensure the plastic capacity of the members is reached. It is known that as the increase thickness of the bracket, the moment transferring capacity is increased simultaneously. However the required quantity of steel is also increased. So stiffeners are more economical on improving the seismic performance of the joints.

5. Conclusions

Based on the experimental and numerical results shown in previous sections, following conclusions can be made:

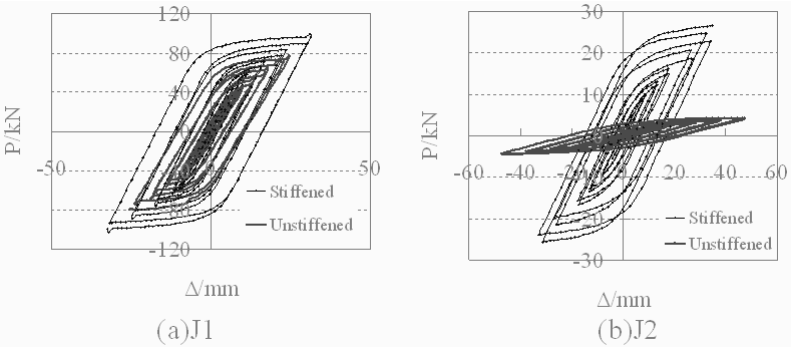

(a)J1 (b)J2

Figure 7 Load versus displacement curves for beams

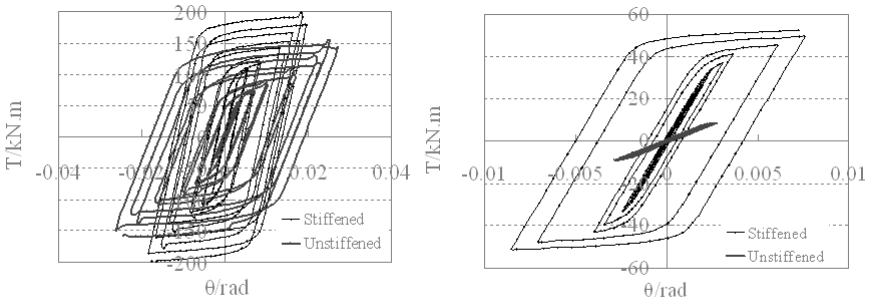

(a)J1 (b)J2

Figure 8 Torque versus rotation curves for brackets

The main factor affecting the seismic performance of the joint is the load bearing capacity ratio Ty/Mp, where Ty is the yield torque of the bracket section and Mp is the plastic moment of the beam section.

FEA results show that the stiffeners have a significant effect on the moment transferring capacity of the joint whose bracket wall is not thick enough to transfer the moment of the beam end. The FEA results also indicate that the energy dissipation capability is improved compared with the unstiffened joints, and the rotation of the bracket is also reduced.

REFERENCES

[1] Kurobane Y, Makino Y, Ochi K. (1984). Ultimate resistance of unstiffened tubular joints. *Journal of Structural Engineering, ASCE* **110:2**, 385–400.

[2] Kurobane Y, Ogawa K. (1993). New criteria for ductility design of joints based on complete CHS truss tests. In: Coutie MG, Davies G, editors. Tubular structures. V. London: Spon E&FN.

[3] Kurobane Y, Ogawa K, Sakae K. Behavior and design of composite lattice girders with concrete slabs. In: Grundy P, Holgate A, Wang B, editors.Tubular structures VI. Rotterdam: Balkema; 1994.

[4] T.Usami, H.B.Ge (1998). Cyclic behavior of thin-walled steel structures-numerical analysis. *Thin Wall-Structures* **32:6**, 41-80.

[5] Wang, W. and Yi-Yi Chen (2007). Hysteretic behaviour of tubular joints under cyclic loading. Journal of *Constructional Steel Research* **63**, 1384–1395.

[6] Elchalakani, M., Zhao, X.L. and Grzebieta, R.H. (2004). Cyclic Bending Tests to Determine Fully Ductile Section Slenderness Limits for Cold-Formed Circular Hollow Sections. *Journal of structural engineering, ASCE*, 103-107.

[7] Elchalakani, M., Zhao, X.L. and Grzebieta, R.H. (2006). Variable amplitude cyclic pure bending tests to determine fully ductile section slenderness limits for cold-formed CHS. *Engineering Structures* **28**, 1223–1235.